Hindawi
Mathematical Problems in Engineering
Volume 2020, Article ID 7343716, 11 pages
https://doi.org/10.1155/2020/7343716

Research Article

Nonlinear Finite Volume Scheme Preserving Positivity for 2D Convection-Diffusion Equations on Polygonal Meshes

Bin Lan [1,2] **and Jianqiang Dong** [3]

[1] *School of Mathematics and Information Science, North Minzu University, Yinchuan 750021, China*
[2] *The Key Laboratory of Intelligent Information and Big Data Processing of Ningxia Province, North Minzu University, Yinchuan 750021, China*
[3] *College of Civil Engineering, Hefei University of Technology, Hefei 230009, China*

Correspondence should be addressed to Bin Lan; lanbin@nun.edu.cn

Received 12 May 2020; Revised 20 July 2020; Accepted 29 July 2020; Published 21 August 2020

Guest Editor: Zaoli Yang

In this paper, a nonlinear finite volume scheme preserving positivity for solving 2D steady convection-diffusion equation on arbitrary convex polygonal meshes is proposed. First, the nonlinear positivity-preserving finite volume scheme is developed. Then, in order to avoid the computed solution beyond the upper bound, the cell-centered unknowns and auxiliary unknowns on the cell-edge are corrected. We prove that the present scheme can avoid the numerical solution beyond the upper bound. Our scheme is locally conservative and has only cell-centered unknowns. Numerical results show that our scheme preserves the above conclusion and has second-order accuracy for solution.

1. Introduction

Convection-diffusion equations are widely used in the fields of solid mechanics, material science, image processing, and so on. So, it is both theoretically and practically important to investigate numerical methods for such equations. An accurate numerical method must maintain the fundamental properties of practical problems. The extremum principle is an important property of solutions for the convection-diffusion equation. It includes minimum principle and maximum principle. The authors of [1, 2] pointed out that the discrete maximum principle (DMP) plays an important role in proving the existence and uniqueness of discrete solution, enforcing numerical stability, and deriving convergence for a sequence of approximate solutions [3]. Pert [4] pointed out that a scheme violating extremum principle can lead to two problems: fully implicit discretization with large time-steps has relatively poor accuracy, and spurious negative values are generated. Moreover, it is proved that a linear operator, resulting from the discretization of diffusion equations, satisfies extremum principle if and only if it is both differential and nonnegativity maintaining.

In general cases, the discrete extremum principle (DEP) is more restrictive than monotonicity (positivity-preserving). However, it is difficult to construct a reliable discretization method that satisfies the DEP on arbitrary convex polygonal meshes. Hence, positivity-preserving is one of the key requirements to discrete schemes for the convection-diffusion equation, which says that it can only guarantee nonnegative bound of the numerical solution. Sheng and Yuan [2] pointed out that the scheme without positivity-preserving can lead to the violation of the entropy constraints of the second law of thermodynamics, causing heat to flow from regions of lower temperature to higher temperature. In regions of large temperature variations, this can cause the temperature to become negative.

The finite volume methods (FVM) guarantee the local conservation. But many classical schemes fail to maintain positivity for strong anisotropic diffusion tensors or on distorted meshes [5–8]. Some nonlinear methods have been developed [9–21] for general diffusion or convection-

diffusion equations, which guarantee the positivity on general or distorted meshes for general tensor coefficients.

Bertolazzi and Manzini [22] proposed a MUSCL-like cell-centered finite volume method, where the discretization of advective fluxes is based on a least-square reconstruction of the vertex values from cell averages. Lipnikov et al. [23] proposed a new slope limiting technique based on a specially minimal nonlinear correction, which follows the ideas of the monotonic upstream-centered scheme for conservation laws (MUSCL). Then, in the studies by Wang et al. and Zhang et al. [16, 24], the limiting technique is used to avoid nonphysical oscillation. In the study by Lan et al. [21], a new upwind scheme is used to discretize the convective flux, and the method did not introduce any slope limiting technique.

In this paper, we develop a nonlinear FV scheme, which satisfies DEP for convection-diffusion problems on arbitrary convex polygonal meshes. Following the idea of the discretization for diffusive flux [18] and convective flux [21], the adaptive approach of choosing stencil is applied. Positivity-preserving scheme can only guarantee nonnegative bound of the numerical solution. Considering that the computation of value on the cell edge and the value of cell-centered unknowns may be out of bound, a correcting technique is introduced. Our scheme is constructed by a nonlinear combination technique and has second-order accuracy for the solution and first-order for the flux.

The article is organized as follows. The model problem is described, and some notations are introduced in Section 2. The main process of construction for the 2D steady convection-diffusion equation is given in Section 3. In Section 4, several numerical tests are exhibited to illustrate the features of our scheme. At last, some conclusions are given in Section 5.

2. The Problem and Notation

Consider the following stationary convection-diffusion problem for unknown function $u = u(x)$:

$$-\nabla \cdot (\kappa \nabla u - \overrightarrow{v} u) = f, \quad \text{in } \mathbf{\Omega}, \tag{1}$$

$$u = g, \quad \text{on } \partial\Omega, \tag{2}$$

where Ω is a bounded polygonal domain in $\mathbb{R} \times \mathbb{R}$ with boundary $\partial\mathbf{\Omega}$, $\kappa = \kappa(x)$ is a known diffusive coefficient, and $\overrightarrow{v} = \overrightarrow{v}(x)$ is a velocity vector field.

Assume that the functions $\overrightarrow{v}(x)$, $f(x)$, and $g(x)$ satisfy the constraints listed as follows:

$$\begin{aligned} \nabla \cdot \overrightarrow{v} \geq 0, \quad & \overrightarrow{v} \in C^1(\overline{\Omega})^2, \\ & f \in L^2(\Omega), \\ & g \in H^{1/2}(\partial\Omega) \cap C(\partial\Omega), \end{aligned} \tag{3}$$

and there are two positive constants λ_1 and λ_2 such that

$$\lambda_1 |\xi|^2 \leq \kappa(x)\xi \cdot \xi \leq \lambda_2 |\xi|^2, \quad \forall \xi \in \mathbb{R} \times \mathbb{R}. \tag{4}$$

The solvability of the problem (1)-(2) has been given, and the maximum and minimum principle can be found in the study by Gilbarg and Trudinger [25].

We use a mesh on Ω made up of arbitrary convex polygon cells. The set of all cells, edges, and nodes are denoted by $\mathcal{T}$, ε, and $\mathcal{N}$, respectively.

We denote the cell by $K, L, \ldots,$ and the cell center is also denoted by $K, L, \ldots,$. In addition, the common edge of two cells K and L is denoted by σ, i.e., $\sigma = K|L \in \mathrm{E}$. The cell-edge σ is also denoted by AB, and the midpoint of σ is denoted by M. Moreover, we denote P_1 and P_2 are two adjacent midpoints of cell K (Figure 1).

Let $\overrightarrow{n}_{K,\sigma}$ (or $\overrightarrow{n}_{L,\sigma}$) be the unit outer normal vector on the cell-edge σ of cell K (or L), κ^T be the transpose of matrix κ, and $\mathscr{E}_K$ be the set of all edges of cell K. Denote $\varepsilon_{\text{int}} = \varepsilon \cap \Omega$ and $\varepsilon_{ext} = \varepsilon \cap \partial\Omega$. Denote $h = (\sup_{K \in \mathcal{T}} m(K))^{1/2}$, where $m(K)$ is the area of cell K.

Integrating (1) over the cell K, we obtain

$$\sum_{\sigma \in \mathrm{E}_K} \left(\mathscr{F}_{K,\sigma} + \mathscr{G}_{K,\sigma} \right) = \int_K f(x) \mathrm{d}x, \tag{5}$$

where the diffusive and convective flux are defined as

$$\mathscr{F}_{K,\sigma} = -\int_\sigma \nabla u(x) \cdot \kappa^T(x) \overrightarrow{n}_{K,\sigma} \mathrm{d}l, \tag{6}$$

$$\mathscr{G}_{K,\sigma} = \int_\sigma \overrightarrow{v} u(x) \cdot \overrightarrow{n}_{K,\sigma} \mathrm{d}l. \tag{7}$$

3. Construction of the Scheme

3.1. The Diffusive Flux. Following the idea in the study by Sheng and Yuan [18], the adaptive approach of choosing stencil is applied for the approximation of the diffusive flux (equation (6)) together with a nonlinear combination technique. In the method, the two nonnegative parameters are introduced to define a nonlinear two-point flux. Then, the continuity of normal flux on the cell edge is used to give the final discretization of the diffusive flux. At last, the continuity of normal flux is used to obtain the value of u_M. First, we give a brief review of the construction.

Figure 1 shows that a ray originating at the point K along the direction $\kappa^T \overrightarrow{n}_{K,\sigma}$ must intersect one segment connecting two neighboring midpoints of edge of cell K, where the two midpoints are denoted by P_1 and P_2, and the cross point is denoted by O_1. Similarly, a ray originating at the midpoint M along the direction $-\kappa^T \overrightarrow{n}_{K,\sigma}$ must intersect one certain KP_4, where P_4 must be one vertex of σ, and the cross point is denoted by O_2.

Let $\overrightarrow{t}_{KP_1}$, $\overrightarrow{t}_{KP_2}$, $\overrightarrow{t}_{MK}$, and $\overrightarrow{t}_{MP_4}$ be some unit tangential vectors along their corresponding directions, respectively. $\theta_i (i = 1, \ldots, 4)$ are some corresponding angles. Hence, we established the following relations:

$$\frac{\kappa^T \overrightarrow{n}_{K,\sigma}}{\left| \kappa^T \overrightarrow{n}_{K,\sigma} \right|} = \frac{\sin\theta_2}{\sin(\theta_1 + \theta_2)} \overrightarrow{t}_{KP_1} + \frac{\sin\theta_1}{\sin(\theta_1 + \theta_2)} \overrightarrow{t}_{KP_2}, \tag{8}$$

$$-\frac{\kappa^T \overrightarrow{n}_{K,\sigma}}{\left| \kappa^T \overrightarrow{n}_{K,\sigma} \right|} = \frac{\sin\theta_4}{\sin(\theta_3 + \theta_4)} \overrightarrow{t}_{MK} + \frac{\sin\theta_3}{\sin(\theta_4 + \theta_4)} \overrightarrow{t}_{MP_4}. \tag{9}$$

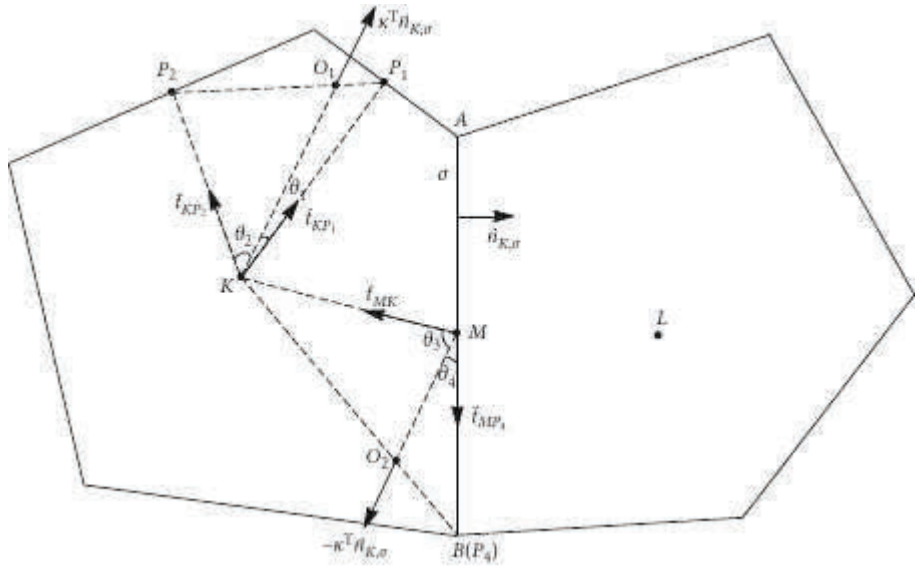

Figure 1: Local stencil 1.

Substituting equation (8) into equation (6) and neglecting the high-order terms, we have

$$\begin{aligned}\overline{F}_1 &= -\left|\kappa_K^T \vec{n}_{K,\sigma}\right\|\sigma\left|\left(\frac{\sin\theta_2}{\sin(\theta_1+\theta_2)}\frac{u_{P_1}-u_K}{|KP_1|}+\frac{\sin\theta_1}{\sin(\theta_1+\theta_2)}\frac{u_{P_2}-u_K}{|KP_2|}\right)\right.\\ &= a_1\left(u_K-u_{P_1}\right)+a_2\left(u_K-u_{P_2}\right),\end{aligned} \tag{10}$$

where

$$\begin{aligned}a_1 &= \frac{\left|\kappa_K^T \vec{n}_{K,\sigma}\right\|\sigma|}{|KP_1|}\frac{\sin\theta_2}{\sin(\theta_1+\theta_2)},\\ a_2 &= \frac{\left|\kappa_K^T \vec{n}_{K,\sigma}\right\|\sigma|}{|KP_1|}\frac{\sin\theta_1}{\sin(\theta_1+\theta_2)}.\end{aligned} \tag{11}$$

Similarly, substituting equation (9) into equation (6), we have

$$\begin{aligned}\overline{F}_2 &= \left|\kappa_K^T \vec{n}_{K,\sigma}\right\|\sigma\left|\left(\frac{\sin\theta_4}{\sin(\theta_3+\theta_4)}\frac{u_K-u_M}{|MK|}+\frac{\sin\theta_3}{\sin(\theta_3+\theta_4)}\frac{u_{P_4}-u_M}{|MP_4|}\right)\right.\\ &= a_3\left(u_K-u_M\right)+a_4\left(u_{P_4}-u_M\right),\end{aligned} \tag{12}$$

where

$$\begin{aligned}a_3 &= \frac{\left|\kappa_K^T \vec{n}_{K,\sigma}\right\|\sigma|}{|MK|}\frac{\sin\theta_4}{\sin(\theta_3+\theta_4)},\\ a_4 &= \frac{\left|\kappa_K^T \vec{n}_{K,\sigma}\right\|\sigma|}{|MP_4|}\frac{\sin\theta_3}{\sin(\theta_3+\theta_4)}.\end{aligned} \tag{13}$$

Combined with equations (10)–(12), the discrete normal flux on σ can be defined as follows:

$$\begin{aligned}F_{K,\sigma} &= \mu_1\overline{F}_1+\mu_2\overline{F}_2 = \mu_1 a_1\left(u_K-u_{P_1}\right)+\mu_1 a_2\left(u_K-u_{P_2}\right)\\ &\quad+\mu_2 a_3\left(u_K-u_M\right)+\mu_2 a_4\left(u_{P_4}-u_M\right),\end{aligned} \tag{14}$$

where μ_1 and μ_2 are some nonlinear coefficients with $\mu_1+\mu_2=1$, which will be given later.

In order to assure μ_1 and μ_2 are positive, two additional parameters ω_1 and ω_2 are introduced later. According to the different positions of P_1 and P_2, three cases exist.

We assume that $u_{P_1}\neq u_M$ and $u_{P_2}\neq u_M$, the normal flux (14) can be rewritten as

$$\begin{aligned}F_{K,\sigma} &= \left(\mu_1\left(a_1+a_2\right)+\mu_2 a_3\right)u_K-\mu_2\left(a_3+a_4\right)u_M\\ &\quad-\mu_1\left(a_1u_{P_1}+a_2u_{P_2}\right)+\mu_2 a_4u_{P_4}\\ &= \left(\mu_1\left(a_1+a_2\right)\left(1+\omega_1\right)+\mu_2 a_3\right)u_K\\ &\quad-\mu_2\left(a_3+a_4\left(1+\omega_2\right)\right)u_M\\ &\quad-\mu_1\left(a_1\left(u_{P_1}+\omega_1u_K\right)+a_2\left(u_{P_2}+\omega_1u_K\right)\right)\\ &\quad+\mu_2 a_4\left(u_{P_4}+\omega_2u_M\right).\end{aligned} \tag{15}$$

In order to obtain the two-point flux approximation, the last two terms of the above expression should vanish; hence, μ_1 and μ_2 are given as follows:

$$\begin{aligned}\mu_1 &= \frac{a_4\left(u_{P_4}+\omega_2u_M\right)}{a_1\left(u_{P_1}+\omega_1u_K\right)+a_2\left(u_{P_2}+\omega_1u_K\right)+a_4\left(u_{P_4}+\omega_2u_M\right)},\\ \mu_2 &= \frac{a_1\left(u_{P_1}+\omega_1u_K\right)+a_2\left(u_{P_2}+\omega_1u_K\right)}{a_1\left(u_{P_1}+\omega_1u_K\right)+a_2\left(u_{P_2}+\omega_1u_K\right)+a_4\left(u_{P_4}+\omega_2u_M\right)}.\end{aligned} \tag{16}$$

Hence, (15) can be expressed as follows:

$$F_{K,\sigma} = A_{K,\sigma,1}u_K-A_{K,\sigma,2}u_M, \tag{17}$$

where

$$A_{K,\sigma,1} = \mu_1 (a_1 + a_2)(1 + \omega_1) + \mu_2 a_3,$$
$$A_{K,\sigma,2} = \mu_2 (a_3 + a_4(1 + \omega_2)). \tag{18}$$

In order to assure $\mu_1 > 0$ and $\mu_2 > 0$, two parameters ω_1 and ω_2 can be chosen such that

$$a_1\left(u_{P_1} + \omega_1 u_K\right) + a_2\left(u_{P_2} + \omega_1 u_K\right) \geq 0,$$
$$a_4\left(u_{P_4} + \omega_2 u_M\right) \geq 0. \tag{19}$$

If

$$a_1\left(\left(u_{P_1} + \omega_1 u_K\right) + a_2\left(u_{P_2} + \omega_1 u_K\right)\right.$$
$$= a_4\left(u_{P_4} + \omega_2 u_M\right) = 0. \tag{20}$$

We let $\mu_1 = \mu_2 = (1/2)$.

If $u_{P_1} = u_M$ or $u_{P_2} = u_M$, equation (14) can be expressed in the similar form (17) by using the above method.

Similarly, on the edge σ of the cell L, we have

$$F_{L,\sigma} = A_{L,\sigma,1} u_L - A_{L,\sigma,2} u_M. \tag{21}$$

Using the continuity of normal flux $F_{K,\sigma} + F_{L,\sigma} = 0$ on edge σ, we obtain

$$u_M = \frac{A_{K,\sigma,1} u_K + A_{L,\sigma,1} u_L}{A_{K,\sigma,2} + A_{L,\sigma,2}}. \tag{22}$$

Substitute equation (22) into equation (17) to obtain the nonlinear two-point diffusive flux on $\sigma = K|L$:

$$F_{K,\sigma} = A_{K,\sigma} u_K - A_{L,\sigma} u_L, \tag{23}$$

where $A_{K,\sigma} = A_{K,\sigma,1} A_{L,\sigma,2} / A_{K,\sigma,2} + A_{L,\sigma,2}$, and $A_{L,\sigma} = A_{K,\sigma,2} A_{L,\sigma,1} / A_{K,\sigma,2} + A_{L,\sigma,2}$.

From the computation of vertex unknowns, a method with second-order accuracy has been proposed in the study by Sheng and Yuan [26]. We know that $u_M > 0$ as long as $u_K > 0$ and $u_L > 0$ in equation (22).

3.2. The Convective Flux. We focus on the expression of convective flux in equation (7) for $\forall \sigma = K|L \in \varepsilon_{\text{int}}$ and obtain

$$\mathcal{G}_{K,\sigma} = u_M \int_\sigma \vec{v} \cdot \vec{n}_{K,\sigma} dl + O\left(h^2\right)$$
$$= u_M\left(v^+_{K,\sigma} - v^-_{K,\sigma}\right) + O\left(h^2\right), \tag{24}$$

where u_M is the value of midpoint M on the cell-edge σ, and

$$v^+_{K,\sigma} = \frac{1}{2}\left(\left|v_{K,\sigma}\right| + v_{K,\sigma}\right),$$
$$v^-_{K,\sigma} = \frac{1}{2}\left(\left|v_{K,\sigma}\right| - v_{K,\sigma}\right), \tag{25}$$
$$v_{K,\sigma} = \int_\sigma v \cdot \vec{n}_{K,\sigma} dl.$$

In order to ensure that the discretization of equation (24) has the same structure as the scheme (23), we divide the integral term into positive part ($v^+_{K,\sigma}$) and negative part ($v^-_{K,\sigma}$). Moreover, the property of upwind is also considered.

Neglecting the high-order terms, we have the following approximate expression of the upwind formula [27]:

$$\mathcal{G}_{K,\sigma} \approx u_M\left(v^+_{K,\sigma} - v^-_{K,\sigma}\right). \tag{26}$$

In order to approximate the continuous flux $\mathcal{G}_{K,\sigma}$ on the cell-edge σ with second-order accuracy, we propose the following method.

A local stencil is given in Figure 2. For the cell K, M is the midpoint of an arbitrary edge and M_1, M_2 are the other two midpoints adjacent to it. We denote $S_{\triangle MM_1K}$ be the area of triangle MM_1K and define

$$\overline{u}_K = \sum_{M \in \sigma, \sigma \in \mathcal{E}_K} \omega_M u_M, \tag{27}$$

where $\omega_M = ((S_{\triangle MM_1K} + S_{\triangle KM_2M})^{-1} / \sum_{M \in \sigma, \sigma \in \varepsilon_K} (S_{\triangle MM_1K} + S_{\triangle KM_2M})^{-1})$. For a special case (Figure 3), we set the cell K as a triangle and define $\overline{u}_K = \omega_M u_M + \omega_{M_1} u_{M_1} + \omega_{M_2} u_{M_2}$, where

$$\omega_M = \frac{s_1}{s},$$
$$\omega_{M_1} = \frac{s_2}{s},$$
$$\omega_{M_2} = \frac{s_3}{s},$$
$$s = s_1 + s_2 + s_3,$$
$$s_1 = \left(S_{\triangle MM_1K} + S_{\triangle KM_2M}\right)^{-1},$$
$$s_2 = \left(S_{\triangle MM_1K} + S_{\triangle KM_1M_2}\right)^{-1}, \tag{28}$$
$$s_3 = \left(S_{\triangle KM_1M_2} + S_{\triangle MKM_2}\right)^{-1}.$$

It is obvious that $\overline{u}_K$ is a second-order approximation to u_K, i.e., $|u(K) - \sum_{M \in \sigma, \sigma \in \mathcal{E}_K} \omega_M u(M)| = O(h^2)$ if the solution $u \in C^2(K)$.

Then, the approximation of $\mathcal{G}_{K,\sigma}$ on cell-edge σ can be defined as follows.

For $\sigma \in \mathcal{E}_{\text{int}}$, we define

$$G_{K,\sigma} = B_{K,\sigma} u_K - B_{L,\sigma} u_L, \tag{29}$$

where

$$B_{K,\sigma} = \frac{v^+_{K,\sigma} u_M}{\overline{u}_K} \geq 0,$$
$$B_{L,\sigma} = \frac{v^+_{L,\sigma} u_M}{\overline{u}_L} \geq 0. \tag{30}$$

For $\sigma \in \mathcal{E}_{ext}$, we define

$$G_{K,\sigma} = B_{K,\sigma} u_K - b_{K,\sigma}, \tag{31}$$

where

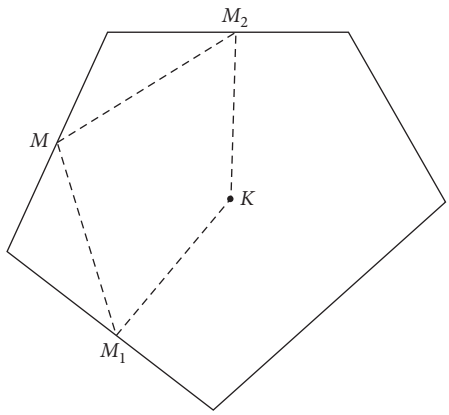

Figure 2: Local stencil 2.

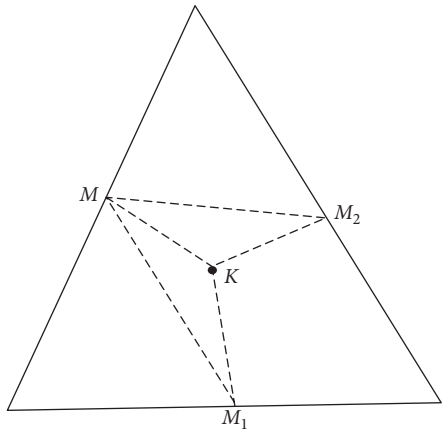

Figure 3: Local stencil of triangle.

$$B_{K,\sigma} = \frac{v^{+}_{K,\sigma} u_M}{\overline{u}_K} \geq 0,$$
$$b_{K,\sigma} = v^{-}_{K,\sigma} g_M. \tag{32}$$

3.3. The Finite Volume Scheme and Picard Iteration. By using the definition of discretization of diffusive and convective flux, the finite volume scheme can be constructed as follows:

$$\sum_{\sigma \in \varepsilon_K} \left(F_{K,\sigma} + G_{K,\sigma}\right) = |K| F_K + \sum_{\sigma \in \varepsilon_K \cap \varepsilon_{ext}} \left(A_{K,\sigma,2} u_M + b_{K,\sigma}\right), \quad K \in \mathcal{J}. \tag{33}$$

$$u_{M_i} = g_{M_i}, \quad \forall M_i \in \partial\Omega, \tag{34}$$

where $f_K = f(K)$ and $g_{M_i} = g(x_{M_i})$.

Let U be the discrete unknown vector and $A(U)$ be the coefficient matrix. A nonlinear algebraic system of the schemes (33) and (34) can be formed: $A(U)U = F$. The $A(U)$ is assembled by the coefficients of diffusive term $F_{K,\sigma}$ and convective term $G_{K,\sigma}$. We use the Picard nonlinear iteration method to solve the system: choose a small value $\mathscr{E}_{\text{non}} > 0$ and initial vector $U^0 > 0$ and repeat for nonlinear iteration index $s = 1, 2, \ldots,$:

(1) Solve $A(U^{(s-1)})U^{(s)} = F$

(2) Stop if $\|A(U^{(s)})U^{(s)} - F\|_2 \leq \mathrm{E}_{\text{non}} \|A(U^{(0)})U^{(0)} - F\|_2$

The linear algebraic system with coefficient matrix $A(U^{(s-1)})$ is solved by the biconjugate gradient stabilized (BiCGSTab) method, and the linear iterations are terminated when relative norm of the initial residual becomes smaller than ε_{lin}.

3.4. The Algorithm. In this subsection, we describe the detailed algorithm.

Step 1. Initialize $U^{(0)} > 0$, ε_{non}, and ε_{lin}.

Step 2. When $s = 0$,

(a) compute $A^{(0)}_{K,\sigma}$ and $B^{(0)}_{K,\sigma}$;
(b) compute initial residual $\|A(U^{(0)})U^{(0)} - F\|_2$.

Step 3. When $s = 1, 2, \ldots,$

(a) solve $A(U^{(s-1)})U^{(s)} = F$;
(b) correct $U^{(s)}$, see Remark 1;
(c) compute $u^{(s)}_P$ and correct $u^{(s)}_M$, $\forall M \in \sigma, \sigma \in \mathrm{E}, P \in \mathcal{N}$, see Remark 2;
(d) compute $A^{(s)}_{K,\sigma}$ and $B^{(s)}_{K,\sigma}$;
(e) compute residual $\|A(U^{(s)})U^{(s)} - F\|_2$;
(f) whether $\|A(U^{(s)})U^{(s)} - F\|_2 \leq \varepsilon_{\text{non}} \|A(U^{(0)})U^{(0)} - F\|_2$, if true, then go to (Step 4), otherwise, go to (Step 3).

Step 4. Stop.

Remark 1. For $\forall u^{(s)}_K$, if $u^{(s)}_K > \max\left\{u^{(s-1)}_M, M \in \sigma, \sigma \in \mathrm{E}_K\right\}$, let $u^{(s)}_K = \overline{u}^{(s-1)}_K$.

Remark 2. The value of $\forall u^{(s)}_M$ can be obtained by equation (22). If $\forall u^{(s)}_M > \max\left\{u^{(s)}_K, u^{(s)}_L, u^{(s)}_A, u^{(s)}_B\right\}$, where the common edge σ of two cells K and L is also denoted by AB (Figure 1). Let $u^{(s)}_M = u^{(s-1)}_M$.

It should be noted that the algorithm in Remark 1 is important to avoid the numerical solution beyond the upper bound where the numerical results need to depend on nonnegative initial values of nonlinear iteration.

Theorem 1. *Let $F \geq 0$, $U^{(0)} \geq 0$, and linear systems in Picard iterations are solved exactly. Then,*

$$U^{(s)} \geq 0, \quad (s = 1, 2, 3, \ldots,). \tag{35}$$

The detailed proof of positivity is given in the study by Yuan and Sheng [11].

Now, we state our conclusion, which says that our scheme can avoid the numerical solution beyond the upper bound. Denote $u_{\max} = \max\{0, u_K, u_M, \forall K \in \mathcal{T}, \forall M \in \varepsilon\}$.

We assume $u_{K_0} = u_{\max}$. Using Remark 1, we know that $u_{K_0} \leq \max\left\{u_M, M \in \sigma, \sigma \in \varepsilon_{K_0}\right\}$.

4. Numerical Experiments

In order to demonstrate the accuracy and robustness of the scheme, we test several problems and take $\varepsilon_{\text{non}} = 1.0e^{-6}$ and

$\varepsilon_{\text{lin}} = 1.0e^{-10}$. The convergence order can be obtained by the following formula:

$$\text{Order} = \frac{\log\left(\text{Error}\left(N_1\right)/\text{Error}\left(N_2\right)\right)}{\log\left(N_2/N_1\right)}, \tag{36}$$

where N_1 and N_2 represent different number of cells, and $\text{Error}(N_1)$ and $\text{Error}(N_2)$ are the corresponding L_2 errors.

4.1. The Problem with Anisotropic Diffusion Tensor. Consider the problems (1) and (2) with Dirichlet boundary condition on $\Omega = [0,1] \times [0,1]$, and take $v = (-1,1)^T$. The exact solution is

$$u(x,y) = \cos\left(\frac{\pi x}{2}\right)e^y, \tag{37}$$

and the diffusion coefficient is

$$\kappa = \begin{pmatrix} 100\varepsilon & 0 \\ 0 & \varepsilon \end{pmatrix}. \tag{38}$$

First, we test the accuracy of our scheme on random quadrilateral meshes shown in Figure 4. Table 1 gives the corresponding L_2 error and the numbers of nonlinear iteration numbers $it^{\#}_{\text{non}}$ with a different parameter ε. We can see that our scheme obtains second-order accuracy for the solution and at least first-order accuracy for the flux. The average number of nonlinear iterations is 36.8 when $\varepsilon = 10^{-6}$. However, for $\varepsilon = 1.0$, the corresponding number increases while the number of cell increases.

4.2. The Problem with Discontinuous Coefficient. Consider the problems (1) and (2) with Dirichlet boundary condition on $\Omega = [0,1] \times [0,1]$, and take $v = (1,1)^T$. The exact solution is

$$u(x,y) = \begin{cases} \sin\dfrac{\pi}{2}x + \sin\dfrac{\pi}{2}y, & x < \dfrac{1}{2}, \\ \dfrac{\sqrt{2}\,c\pi\left(x - (1/2)\right)}{4} + \sin\dfrac{\pi}{2}y + \dfrac{\sqrt{2}}{2}, & x \geq \dfrac{1}{2}, \end{cases} \tag{39}$$

and the diffusion coefficient is

$$\kappa = \begin{cases} c_0 \times \varepsilon, & x < \dfrac{1}{2}, \\ \varepsilon, & x \geq \dfrac{1}{2}, \end{cases} \tag{40}$$

where $c_0 = 40$.

We test this problem on random triangle meshes shown in Figure 5. The numerical results with a different parameter $\varepsilon = 1.0, 10^{-6}$ are given in Table 2. We can see that our scheme almost obtain second-order accuracy for the solution and at least first-order accuracy for the flux. The average numbers of nonlinear iterations are 25 and 23 for $\varepsilon = 1.0$ and $\varepsilon = 1.0, 10^{-6}$, respectively.

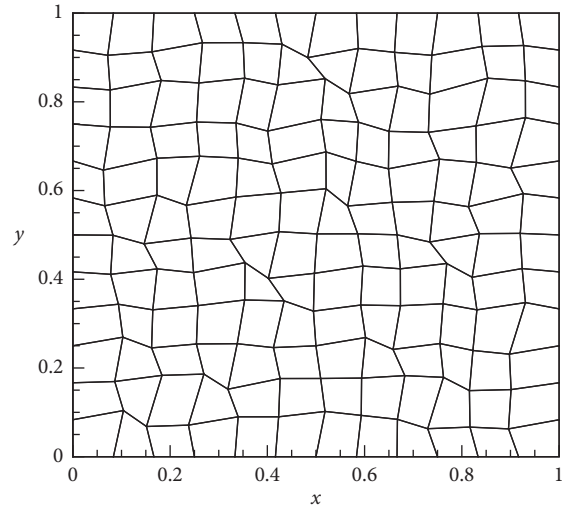

Figure 4: The random quadrilateral meshes.

Then, in order to illustrate the efficiency of our scheme, the comparison of accuracy between the studies by Lan et al. and Zhang et al. [19, 24] and present scheme is given in Table 3. As can be seen from the table, the accuracy is 1.5 in the study by Zhang et al. [24] and more than 2.0 in the study by Lan et al. [19] and our new scheme. However, the computed results in our scheme can approximate the exact solution more well.

4.3. Positivity of Numerical Solutions. Now, we consider the problem (1)-(2) in the unit square $\Omega = [0,1]^2$ with homogeneous Dirichlet boundary conditions. Take $\overrightarrow{v} = (1,1)^T$, and set

$$\kappa = \begin{pmatrix} \cos\theta & \sin\theta \\ -\sin\theta & \cos\theta \end{pmatrix}\begin{pmatrix} k_1 & 0 \\ 0 & k_2 \end{pmatrix}\begin{pmatrix} \cos\theta & -\sin\theta \\ \sin\theta & \cos\theta \end{pmatrix},$$

$$f = \begin{cases} 1, & \text{if } (x,y) \in \left[\dfrac{3}{8},\dfrac{5}{8}\right]^2, \\ 0, & \text{otherwise.} \end{cases} \tag{41}$$

We take $k_1 = 1$, $k_2 = 100$, and $\theta = 5\pi/6$.

The analytical solution $u(x,y)$ is unknown, but the minimum principle states that it is nonnegative. It is a challenging task to solve it accurately because they can result in significant violation of the positivity and even produce a numerical solution with nonphysical oscillations. We will show that our new nonlinear scheme can also obtain the nonnegative solution.

First, we test the new scheme on the random quadrilateral meshes with 128×128 cells. The corresponding distribution is similarly shown in Figure 6), and the numerical solution is given in Figure 7. The minimum value is $u_{\min} = 0$ and the maximum value is $u_{\max} = 6.7603 \times 10^{-4}$, which show that our scheme preserves the positivity of the solution and does not produce any nonphysical oscillations. Then, we test it on the random triangular meshes. The computed results show that $u_{\min} = 0$ and $u_{\max} = 6.7582 \times 10^{-4}$.

Table 1: Accuracy for the problem with anisotropic coefficient.

	Cells	144	576	2304	9216	36864
$\varepsilon = 1.0$	ε_2^u	$3.11E-3$	$7.50E-4$	$2.09E-4$	$5.46E-5$	$1.42E-5$
	Order	—	2.05	1.84	1.94	1.94
	ε_2^F	$1.06E+0$	$3.94E-1$	$1.76E-1$	$8.28E-2$	$3.96E-2$
	Order	—	2.07	1.54	2.03	0.99
	$it_{\text{non}}^{\#}$	55	85	116	126	153
$\varepsilon = 10^{-6}$	ε_2^u	$5.28E-3$	$1.24E-3$	$3.18E-4$	$8.06E-5$	$2.13E-5$
	Order	—	2.09	1.96	1.98	1.92
	ε_2^F	$7.93E-3$	$1.99E-3$	$5.31E-4$	$1.34E-4$	$3.57E-5$
	Order	—	2.07	1.54	2.03	0.99
	$it_{\text{non}}^{\#}$	36	40	36	33	39

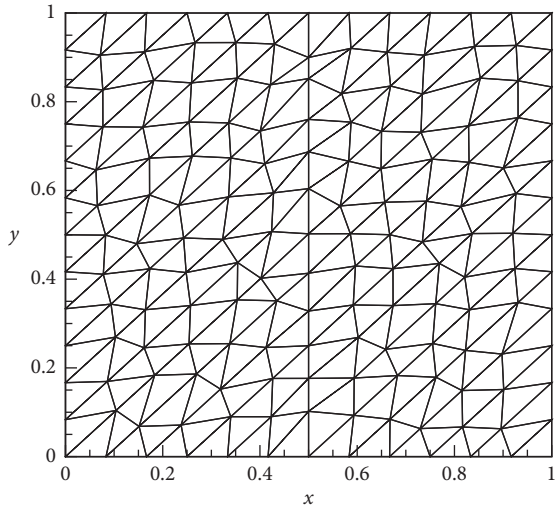

Figure 5: The random triangle meshes.

Table 2: Accuracy for the problem with discontinuous coefficient.

ε	Cells	288	1152	4608	18432	73728
1.0	ε_2^u	$4.87E-4$	$1.39E-4$	$3.82E-5$	$8.68E-6$	$2.13E-6$
	Order	—	1.81	1.86	2.14	2.03
	ε_2^F	$7.83E-2$	$3.04E-2$	$1.39E-2$	$5.51E-3$	$2.50E-3$
	Order	—	2.07	1.54	2.03	0.99
	$it_{\text{non}}^{\#}$	23	24	26	26	26
10^{-6}	ε_2^u	$4.54E-4$	$1.18E-4$	$3.13E-5$	$7.93E-6$	$2.01E-6$
	Order	—	1.94	1.91	1.98	1.98
	ε_2^F	$6.60E-4$	$1.63E-4$	$4.15E-5$	$1.04E-5$	$2.63E-6$
	Order	—	2.07	1.54	2.03	0.99
	$it_{\text{non}}^{\#}$	23	24	23	23	23

These computed results illustrate that our new scheme preserves the positivity of numerical solutions and satisfies the discrete minimum principle.

4.4. Nonphysical Oscillations. We also consider the last nonsmooth anisotropic solution and compute it on the random quadrilateral meshes. Here, we reset $f = 0$. The computational domain is a unit square with a hole, $\Omega = [0,1]^2 \setminus [4/9, 5/9]^2$, so that the boundary $\partial\Omega$ is composed of two disjoint parts Γ_0 and Γ_1 as shown in Figure 8 where the number of cell is 72×72. Γ_0 is the exterior boundary, and Γ_1 is the interior boundary. We set $g = 0$ on Γ_0 and $g = 2$ on Γ_1.

The numerical solutions on the random quadrilateral meshes are shown in Figure 9. The computed results show that $u_{\min} = 6.94E-13$ and $u_{\max} = 1.98$. It means that the minimum 0 is attained on the Γ_0, and the maximum 2 is attained on the Γ_1. So, these computed results illustrate that our scheme can avoid the numerical solution beyond the upper bound and does not produce any nonphysical oscillations.

Then, the computed results without the correct method in Remarks 1 and 2 are shown in Figure 10, and $u_{\min} = 3.87E-6$ and $u_{\max} = 1.91$. However, the numerical oscillations are produced in the computational domain.

Table 3: Comparison of accuracy with discontinuous coefficient ($\varepsilon = 10^{-5}$).

Method	Mesh	Cells	256	1024	4096	16384
Zhang et al. [24]	Uniform	ε_2^u	$1.10E-1$	$3.98E$-2	$1.42E-2$	$5.02E-3$
		Order	—	1.47	1.49	1.50
	Random	ε_2^u	$1.10E-1$	$3.95E$-2	$1.38E-2$	$5.11E-3$
		Order	—	1.48	1.52	1.43
Lan et al. [19]	Uniform	ε_2^u	$4.23E-3$	$9.77E$-4	$2.31E-4$	$5.50E-5$
		Order	—	2.12	2.08	2.07
	Random	ε_2^u	$6.87E-3$	$1.57E$-3	$3.78E-4$	$8.96E-5$
		Order	—	2.13	2.05	2.08
Present	Uniform	ε_2^u	$9.34E-4$	$1.82E-4$	$3.63E-5$	$8.43E-6$
		Order	—	2.36	2.32	2.11
	Random	ε_2^u	$9.16E-4$	$1.89E-4$	$4.04E-5$	$9.85E-6$
		Order	—	2.28	2.23	2.04

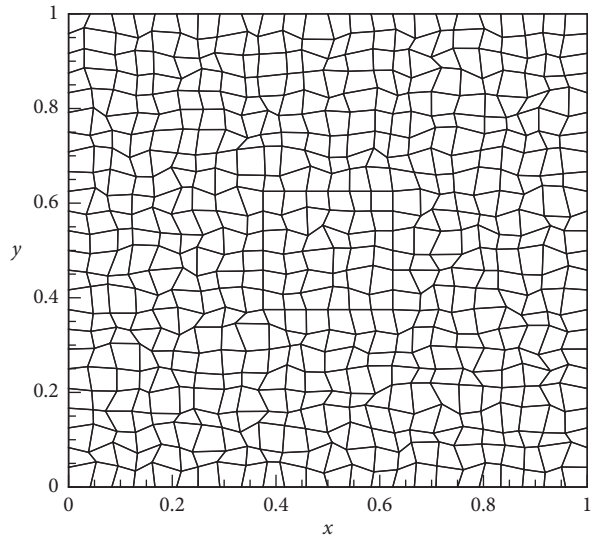

Figure 6: The random quadrilateral meshes.

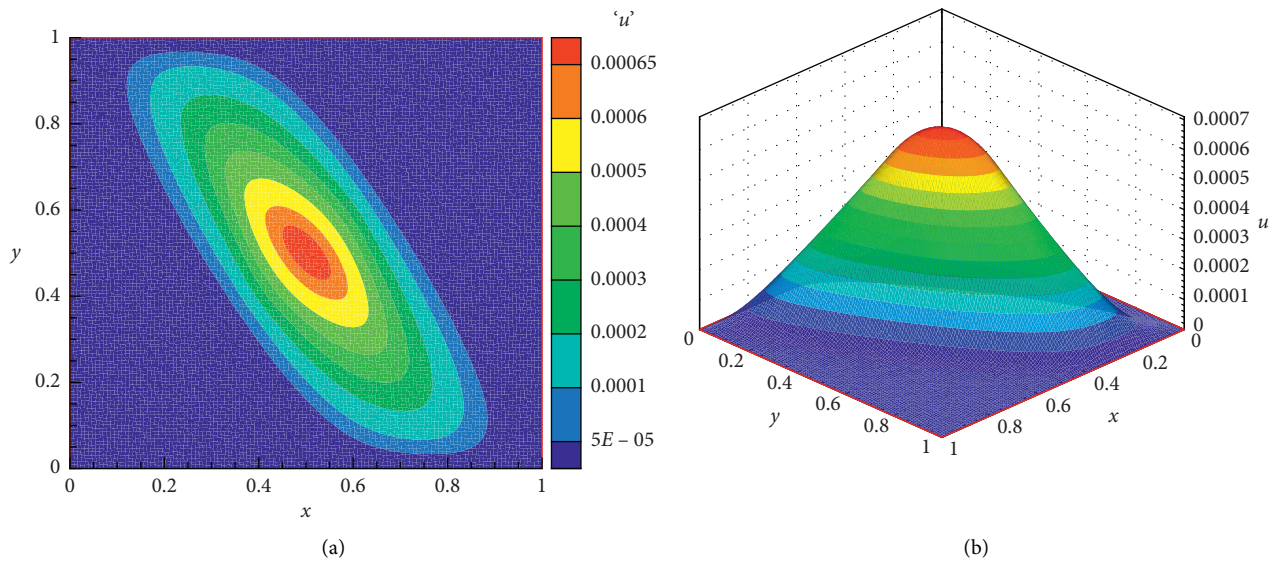

(a) (b)

Figure 7: The numerical solutions on the random quadrilateral meshes.

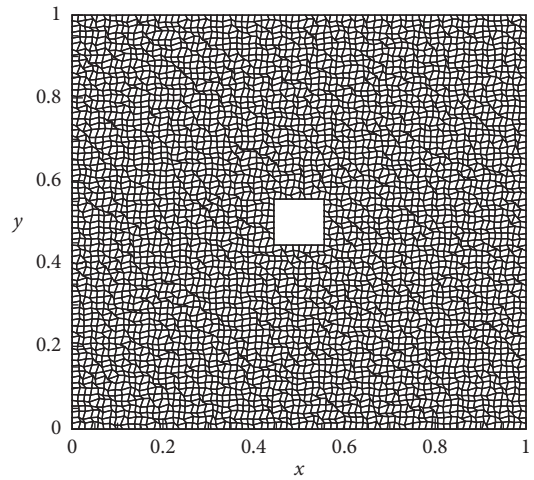

Figure 8: The random quadrilateral meshes with a hole.

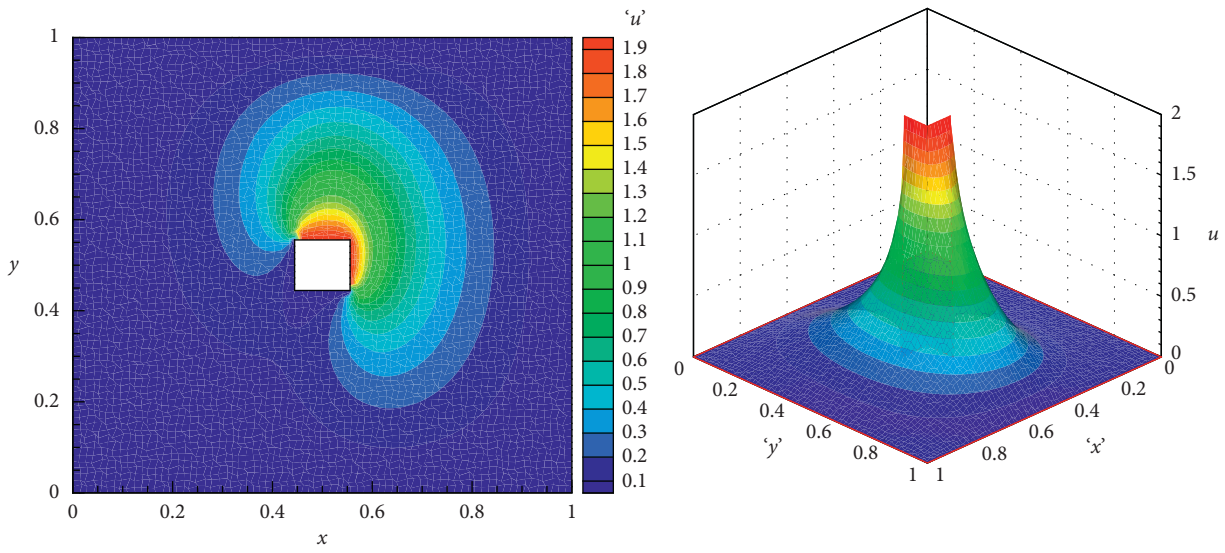

Figure 9: The numerical results on the random quadrilateral meshes.

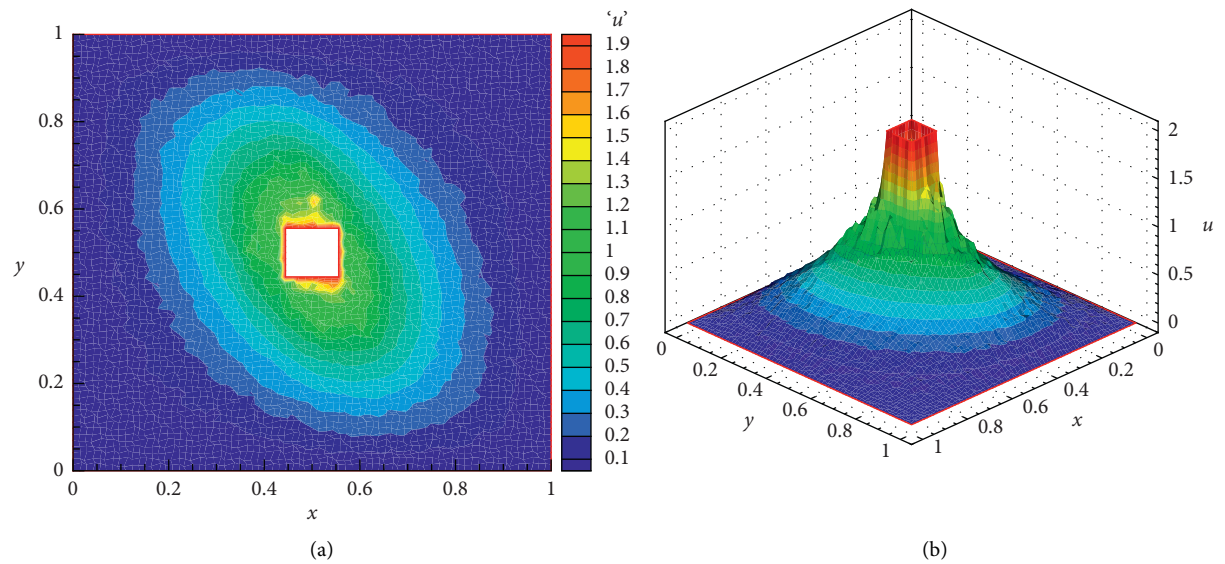

Figure 10: The numerical results without corrections on the random quadrilateral meshes.

5. Conclusion

The aim of this paper is to build a nonlinear finite volume scheme preserving positivity for solving the 2D convection-diffusion equation on arbitrary convex polygonal meshes. We first develop the nonlinear positive finite volume scheme. Then, a corrected method is proposed, and the numerical solution beyond the upper bound can be avoided.

Our scheme includes only cell-centered unknowns. Numerical results show that our new scheme obtains second-order accuracy for the solution and first-order accuracy for the flux. In addition, it can not only keep the positivity but also do not produce any oscillation.

Data Availability

The authors confirm that the data supporting the findings of this study are available within the article (No. 7343716).

Conflicts of Interest

The authors declare that they have no conflicts of interest.

Acknowledgments

This work was partially supported by the Natural Science Foundation of Ningxia (2020AAC03235); General School Level Project (12020000153); National Natural Science Foundation of China (11601013 and 11772165); First-Class Disciplines Foundation of Ningxia (NXYLXK2017B09); and Natural Science Foundation of Ningxia (2020AAC03233).

References

[1] M. G. Edwards and H. Zheng, "A quasi-positive family of continuous Darcy-flux finite-volume schemes with full pressure support," *Journal of Computational Physics*, vol. 227, no. 22, pp. 9333–9364, 2008.

[2] Z. Sheng and G. Yuan, "The finite volume scheme preserving extremum principle for diffusion equations on polygonal meshes," *Journal of Computational Physics*, vol. 230, no. 7, pp. 2588–2604, 2011.

[3] K. Morton, *Numerical Solution of Convection-Diffusion Problems*, Chapman & Hall, London, UK, 1996.

[4] G. J. Pert, "Physical constraints in numerical calculations of diffusion," *Journal of Computational Physics*, vol. 42, no. 1, pp. 20–52, 1981.

[5] J. M. Nordbotten and I. Aavatsmark, "Monotonicity conditions for control volume methods on uniform parallelogram grids in homogeneous media," *Computational Geosciences*, vol. 9, no. 1, pp. 61–72, 2005.

[6] A. Lapin, "Mixed hybrid finite element method for a variational inequality with a quasi-linear operator," *Computational Methods in Applied Mathematics*, vol. 9, no. 4, pp. 354–367, 2009.

[7] H. A. Friis and M. G. Edwards, "A family of MPFA finite-volume schemes with full pressure support for the general tensor pressure equation on cell-centered triangular grids," *Journal of Computational Physics*, vol. 230, no. 1, pp. 205–231, 2011.

[8] K. Lipnikov, G. Manzini, and D. Svyatskiy, "Analysis of the monotonicity conditions in the mimetic finite difference method for elliptic problems," *Journal of Computational Physics*, vol. 230, no. 7, pp. 2620–2642, 2011.

[9] C. Le Potier, "Schéma volumes finis monotone pour des opérateurs de diffusion fortement anisotropes sur des maillages de triangles non structurés," *Comptes Rendus Mathematique*, vol. 341, no. 12, pp. 787–792, 2005.

[10] K. Lipnikov, M. Shashkov, D. Svyatskiy, and Y. Vassilevski, "Monotone finite volume schemes for diffusion equations on unstructured triangular and shape-regular polygonal meshes," *Journal of Computational Physics*, vol. 227, no. 1, pp. 492–512, 2007.

[11] G. Yuan and Z. Sheng, "Monotone finite volume schemes for diffusion equations on polygonal meshes," *Journal of Computational Physics*, vol. 227, no. 12, pp. 6288–6312, 2008.

[12] A. Danilov and Y. Vassilevski, "A monotone nonlinear finite volume method for diffusion equations on conformal polyhedral meshes," *Russian Journal of Numerical Analysis and Mathematical Modelling*, vol. 24, pp. 207–227, 2009.

[13] K. Lipnikov, D. Svyatskiy, and Y. Vassilevski, "Interpolation-free monotone finite volume method for diffusion equations on polygonal meshes," *Journal of Computational Physics*, vol. 228, no. 3, pp. 703–716, 2009.

[14] Z. Sheng, J. Yue, and G. Yuan, "Monotone finite volume schemes of nonequilibrium radiation diffusion equations on distorted meshes," *SIAM Journal on Scientific Computing*, vol. 31, no. 4, pp. 2915–2934, 2009.

[15] Z. Sheng and G. Yuan, "An improved monotone finite volume scheme for diffusion equation on polygonal meshes," *Journal of Computational Physics*, vol. 231, no. 9, pp. 3739–3754, 2012.

[16] S. Wang, G. Yuan, Y. Li, and Z. Sheng, "A monotone finite volume scheme for advection-diffusion equations on distorted meshes," *International Journal for Numerical Methods in Fluids*, vol. 69, no. 7, pp. 1283–1298, 2012.

[17] Z. Sheng and G. Yuan, "A cell-centered nonlinear finite volume scheme preserving fully positivity for diffusion equation," *Journal of Scientific Computing*, vol. 68, no. 2, pp. 521–545, 2016.

[18] Z. Sheng and G. Yuan, "A new nonlinear finite volume scheme preserving positivity for diffusion equations," *Journal of Computational Physics*, vol. 315, pp. 182–193, 2016.

[19] B. Lan, Z. Sheng, and G. Yuan, "A monotone finite volume scheme with second order accuracy for convection-diffusion equations on deformed meshes," *Computer Physics Communication*, vol. 24, pp. 1455–1476, 2018.

[20] B. Lan, Z. Sheng, and G. Yuan, "A new finite volume scheme preserving positivity for radionuclide transport calculations in radioactive waste repository," *International Journal of Heat and Mass Transfer*, vol. 121, pp. 736–746, 2018.

[21] B. Lan, Z. Sheng, and G. Yuan, "A new positive scheme for 2D convection-diffusion equation," *ZAMM-Journal of Applied Mathematics and Mechanics*, vol. 99, pp. 1–13, 2019.

[22] E. Bertolazzi and G. Manzini, "A cell-centered second-order accurate finite volume method for convection-diffusion problems on unstructured meshes," *Mathematical Models and Methods in Applied Sciences*, vol. 14, no. 8, pp. 1235–1260, 2004.

[23] K. Lipnikov, D. Svyatskiy, and Y. Vassilevski, "A monotone finite volume method for advection-diffusion equations on unstructured polygonal meshes," *Journal of Computational Physics*, vol. 229, no. 11, pp. 4017–4032, 2010.

[24] Q. Zhang, Z. Sheng, and G. Yuan, "A finite volume scheme preserving extremum principle for convection-diffusion

equations on polygonal meshes," *International Journal for Numerical Methods in Fluids*, vol. 84, no. 10, pp. 616–632, 2017.

[25] D. Gilbarg and N. Trudinger, *Elliptic Partial Differential Equations of Second Order*, Springer-Verlag, Berlin, Germany, 2001.

[26] Z. Sheng and G. Yuan, "A nine point scheme for the approximation of diffusion operators on distorted quadrilateral meshes," *SIAM Journal on Scientific Computing*, vol. 30, no. 3, pp. 1341–1361, 2008.

[27] B. van Lee, "Towards the ultimate conservative difference scheme. V.A second-order sequel to Godunov's method," *Journal of Computational Physics*, vol. 32, pp. 101–136, 1979.